

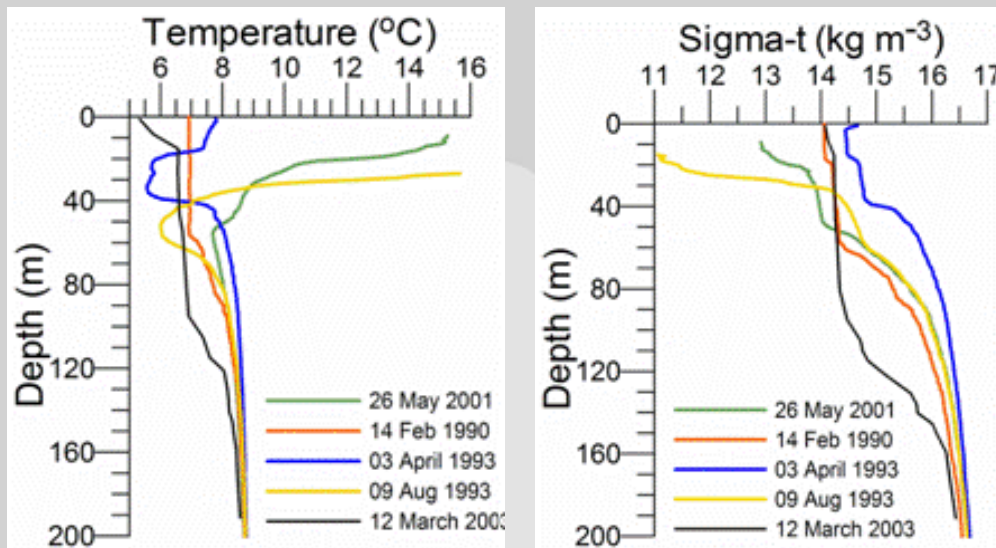
Task II.1. Analysis of available data on the composition of the Black Sea waters

Meeting name: 3rd Regular meeting of the international team of HYSUFCEL
Name, role in the project: Assoc. Prof. Andrea Kellenberger, team member
Institution: University Politehnica Timisoara

Timisoara, 05.11.2013

Vertical stratification of the Black Sea waters into two zones:

- **oxic layer:** an upper layer between 0 - 100 m depth with low density and low salinity
- **anoxic layer:** a bottom layer below 150 m depth with high density and high salinity
- **suboxic layer:** an intermediate zone, with minimal concentrations of O₂ and H₂S



The physical and chemical properties of the Black Sea waters show extreme vertical variations depending on stratification.

Fig. 2. Vertical variation of temperature and conventional density depending on the season [3].

T. Oguz (Ed.), *State of the Environment of the Black Sea (2001 - 2006/7)*, Publications of the Commission on the Protection of the Black Sea against Pollution (BSC) 2008-3, Istanbul, Turkey.

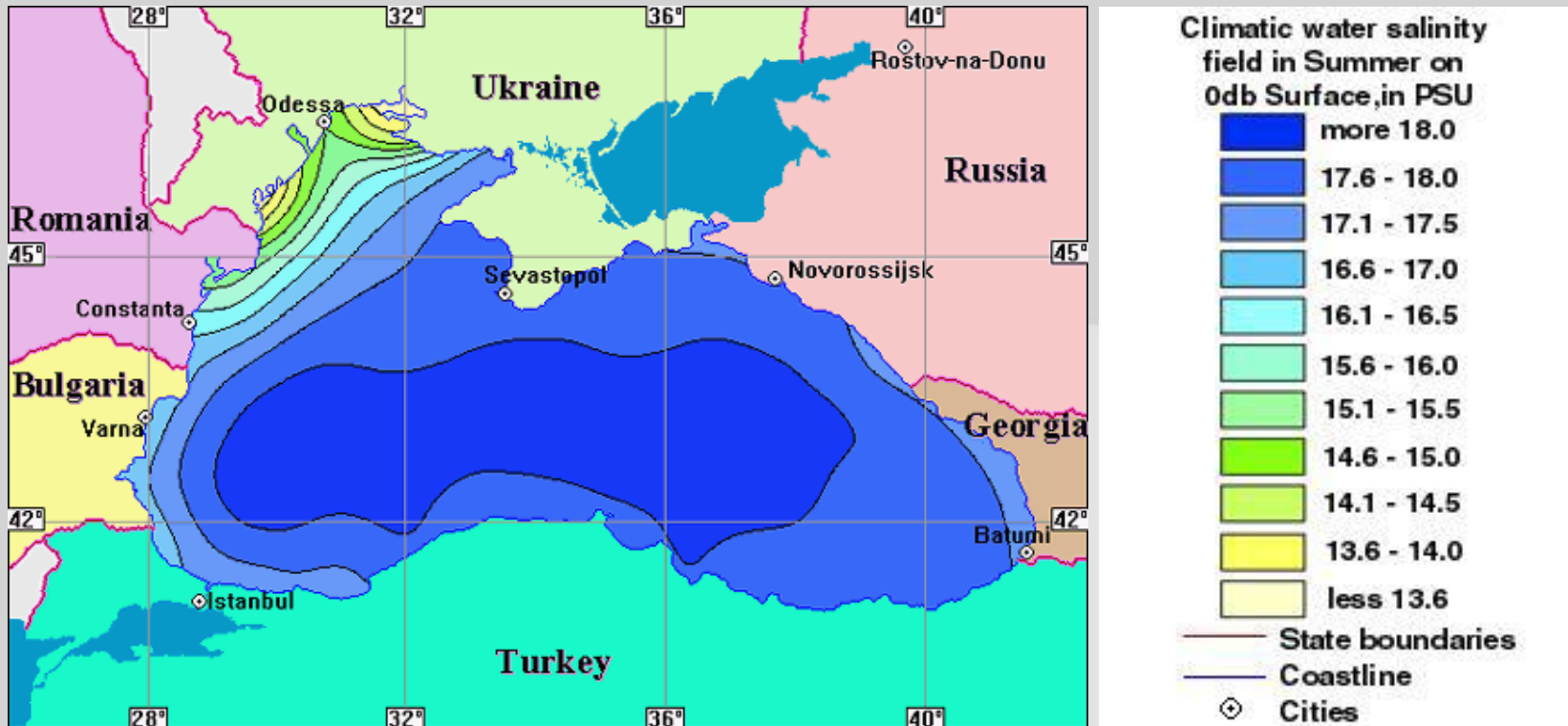
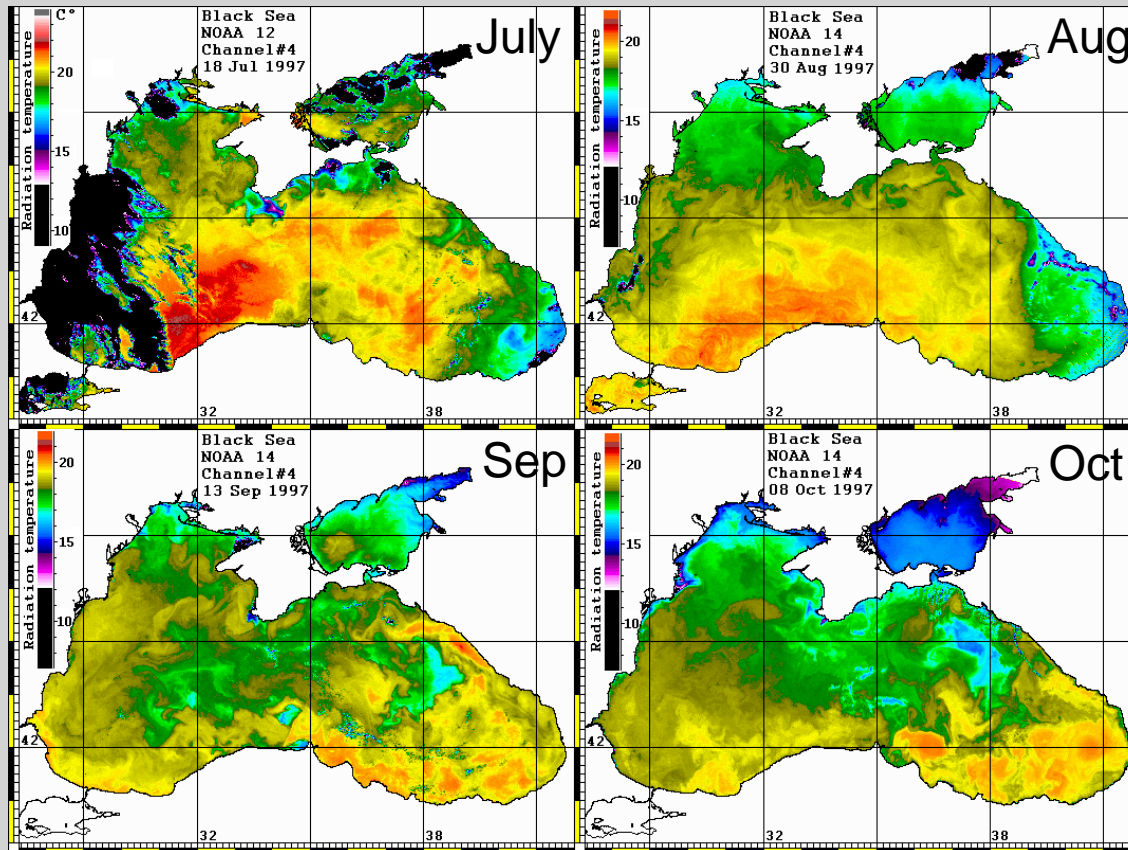


Fig. 3. Variation profile of surface salinity in July [5].

Salinity from 17.1 to 18 ‰, except areas near the mouths of major tributaries, (Danube, Dniester and Dnieper) where salinity values are lower due to important contribution of freshwaters.

<http://www.blackseaweb.net/maps/welcome.html> - accessed 19.11.2012.

Oxic layer – surface water temperature



Winter:

-0.5°C in the north-west
9-10°C in the south-east

Summer:

surface water: 23-26°C
50 and 75 m depth: 7°C

The minimum temperature is not at the basin bottom, but in the layer located between 50-60 m and 80-90 m depth.

Fig. 4. Distribution map of surface temperature of the Black Sea depending on the season [7,8].

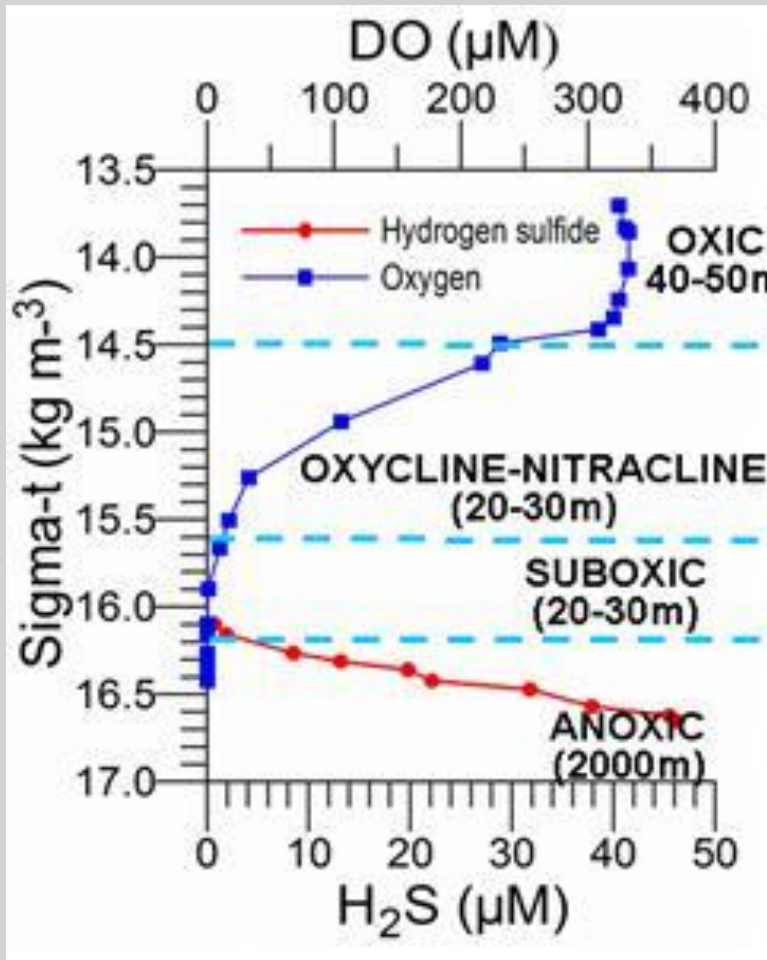
<http://web.deu.edu.tr/atiksu/ana09/ana09.html> - accessed 15.11.2012.

<http://www.blackseaweb.net/satellite/welcome.html> - accessed 15.11.2012.

Oxic layer – oxygen concentration

- Seasonal variations in oxygen concentration are within very large limits between 250-450 μM .
- The highest values of dissolved oxygen concentration are recorded at the end of February, corresponding to the lowest values of surface water temperatures.
- The temperature increase of the surface waters which begins in March, leads to a decrease of the oxygen concentration in the sub-surface layer down to 250 μM .
- Then, depending on the activity of phytoplankton in the summer months, oxygen concentration increases again above 350 μM .

Suboxic layer



The existence of suboxic layer can not be predicted theoretically, given the inverse relationship between oxygen and hydrogen sulfide concentrations. However the suboxic layer exists, with thickness ranging from 20 to 50 m. In the suboxic layer oxygen and hydrogen sulfide concentrations are extremely low, i.e. $\text{O}_2 < 10 \mu\text{M}$ and $\text{H}_2\text{S} < 1 \mu\text{M}$.

Fig. 6. Concentration profiles of O_2 and H_2S versus conventional density in the center of the eastern gyre of the Black Sea during May 2003 [12].

Anoxic layer

- low O_2 concentrations and high conc. of H_2S and sulfides.

- H_2S first occurs at depths of 100 m and its concentration increases sharply in the water column up to 500 m depth. Below this depth its concentration increases much slower, reaching a value of $400 \mu M$ at a depth of 2200 m.

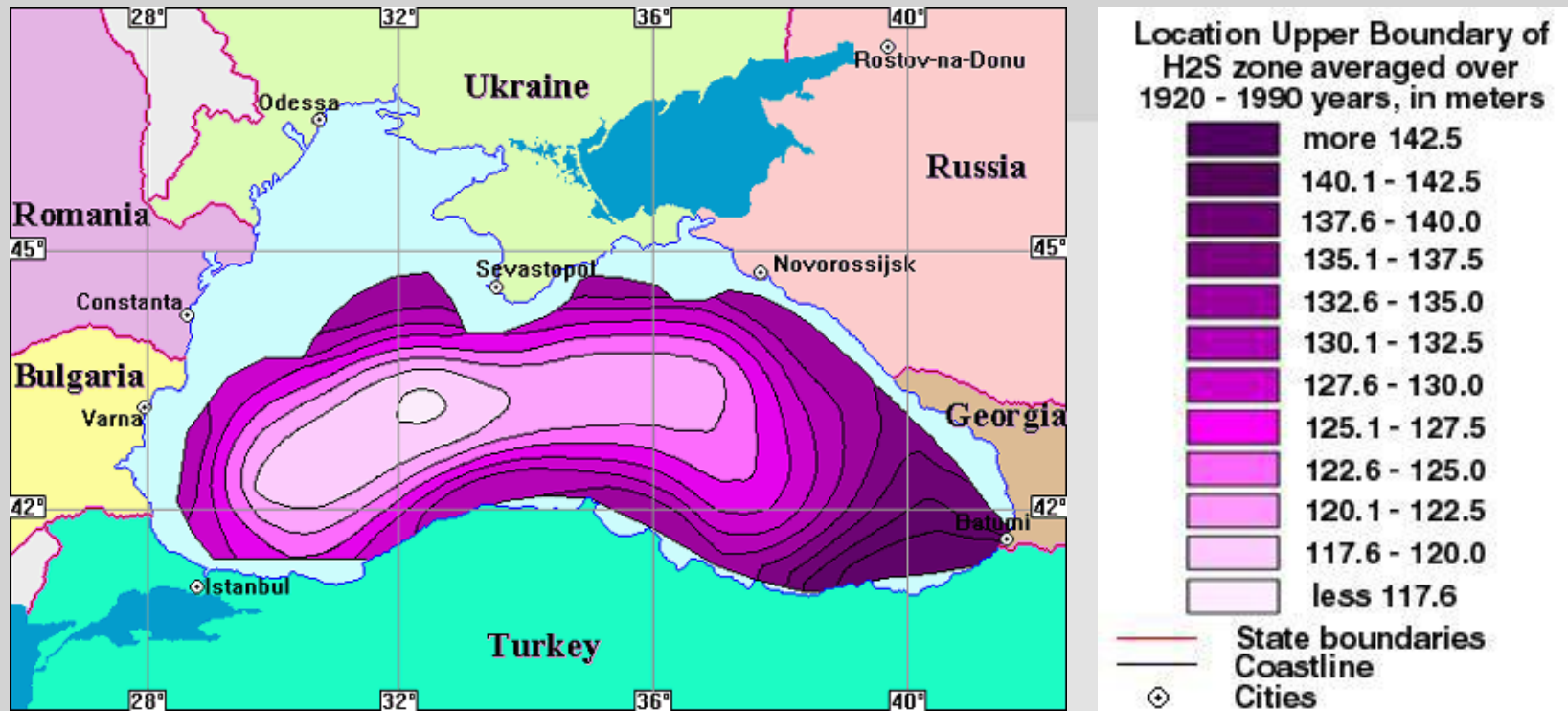


Fig. 10. Location of the upper boundary of H_2S zone averaged over 1920's-1980's [5].

II.1.2. Composition, chemical and physical properties of seawater

Seawater salinity (S) = the total amount of salt in grams dissolved in one kilogram of sea water, considering that bromide and iodide are expressed as chloride, carbonates are converted into oxides and organic substances are fully oxidized.

Chlorinity = the total amount of chlorides, bromides and iodides, expressed in grams contained in one kilogram of sea water, considering that bromide and iodide are expressed as chloride. Chlorinity can be easily determined by titration with silver nitrate.

Seawater density ρ is generally expressed as relative density, relative to the density of distilled water at 4°C, which is equal to unity.

Conventional density σ often used in practice, represents the difference between the density of sea water and fresh water.

$$\sigma = (\rho - 1) \times 1000$$

Table 2. Concentrations of major ions in seawater [26]

Major ion	Salinity S = 35.000‰			
	mg kg S ⁻¹	g kg ⁻¹	mmol kg ⁻¹	mM*
Na ⁺	308.0	10.781	468.96	480.57
K ⁺	11.40	0.399	10.21	10.46
Mg ²⁺	36.69	1.284	52.83	54.14
Ca ²⁺	11.77	0.4119	10.28	10.53
Sr ²⁺	0.227	0.00794	0.0906	0.0928
Cl ⁻	552.94	19.353	545.88	559.40
SO ₄ ²⁻	77.49	2.712	28.23	28.93
HCO ₃ ⁻	3.60	0.126	2.06	2.11
Br ⁻	1.923	0.0673	0.844	0.865
B(OH) ₃	0.735	0.0257	0.416	0.426
F ⁻	0.037	0.00130	0.068	0.070
Total		35.169		

M.E.Q. Pilson, *An introduction to the chemistry of the sea*, Prentice-Hall, New York, 1998.

II.1.3. Composition of artificial seawater

A. Gravimetric salts

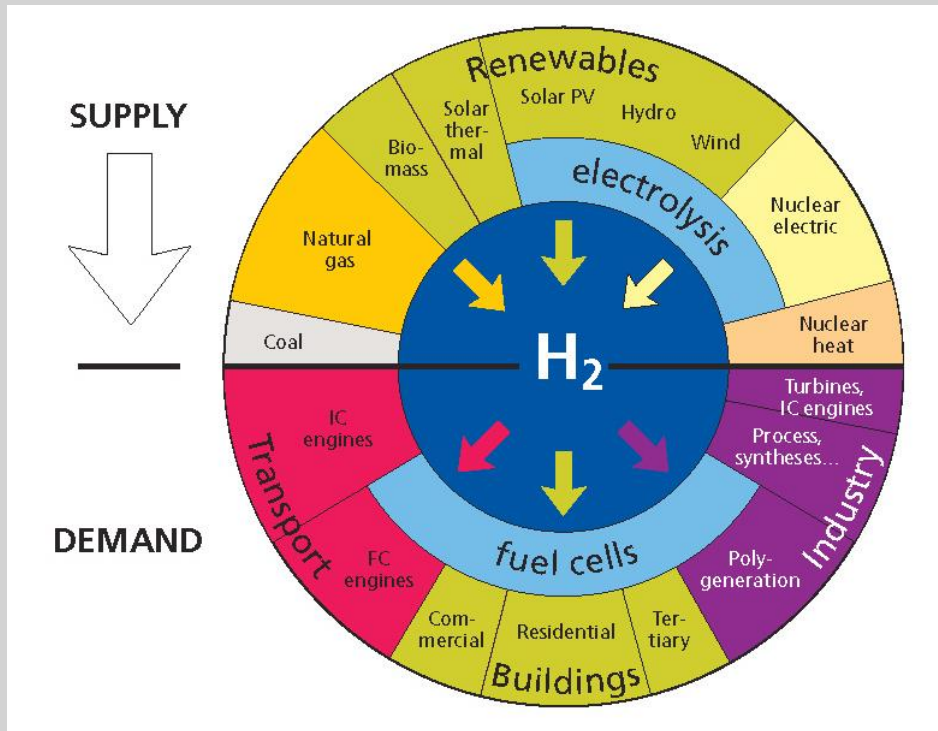
Compound	Molar mass (g mol ⁻¹)	quantity (g kg ⁻¹ solution)	ion	conc. g kg ⁻¹
			Cl ⁻	19.353
NaCl	58.44	23.926	Na ⁺	10.765
Na ₂ SO ₄	142.04	4.008	SO ₄ ²⁻	2.711
KCl	74.56	0.677	K ⁺	0.387
NaHCO ₃	84.00	0.196	HCO ₃ ⁻	0.142
KBr	119.01	0.098	Br ⁻	0.066
H ₃ BO ₃	61.83	0.026	B(OH) ₃	0.026
NaF	41.99	0.003	F ⁻	0.001

B. Volumetric salts

Compound	Molar mass (g mol ⁻¹)	nr. of moles	Stock solution	ρ (g mL ⁻¹)	ion	conc. g kg ⁻¹
MgCl ₂ · 6H ₂ O	203.33	0.05327	1.0 M	1.071	Mg ²⁺	1.295
CaCl ₂ · 2H ₂ O	147.03	0.01033	1.0 M	1.085	Ca ²⁺	0.414
SrCl ₂ · 6H ₂ O	266.64	0.00009	0.1 M	1.013	Sr ²⁺	0.008

C. Distilled water up to 1000.00 g

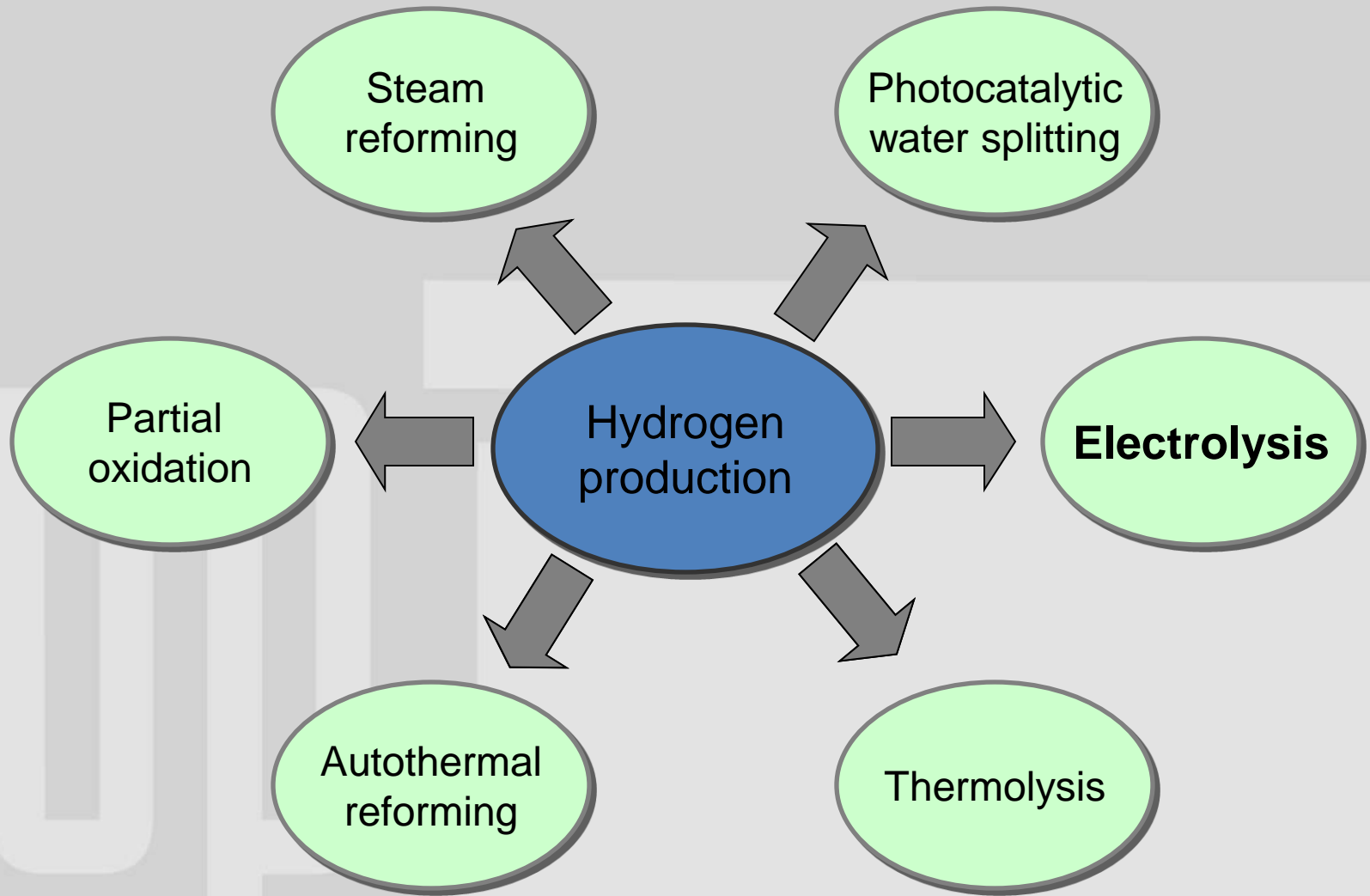
Task II.3. Enhancement of hydrogen evolution reaction on platinum cathode by proton carriers



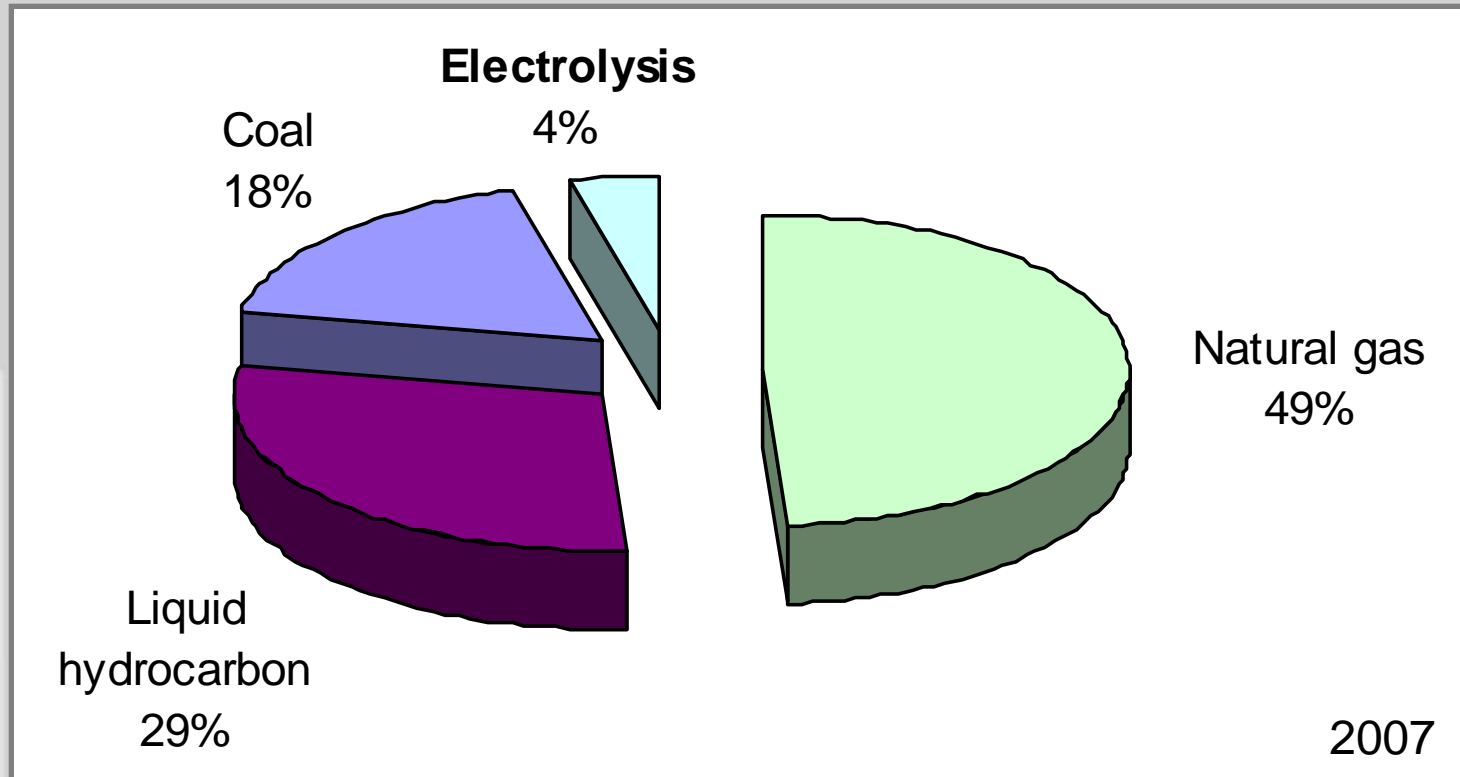
<http://hho-hydrogen-energy.com/html/abouthydrogen.html>

- (1) **hydrogen production** from water using non-renewable energy sources (coal, atomic energy, thermonuclear energy) and renewable energy sources (sun, hydro, wind, currents, tides, biomass).
- (2) **hydrogen delivery**, transportation and storage.
- (3) **hydrogen utilization** in industry, transport (land, water and air) and home.
- (4) problems of **material reliability** and system safety.

Hydrogen production

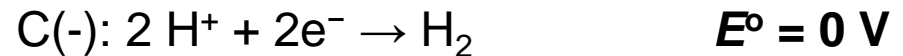
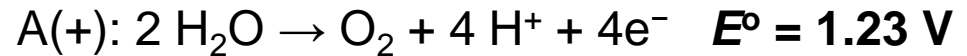
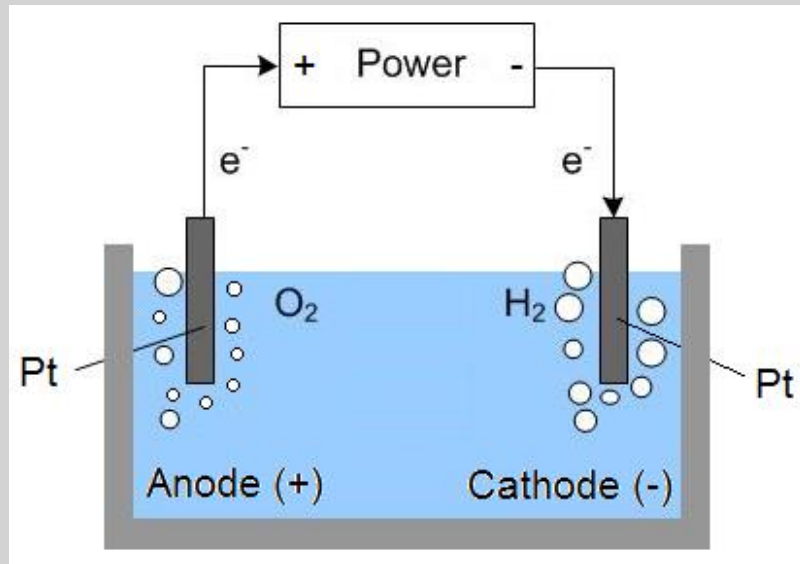


Hydrogen production sources



Water electrolysis

1800: William Nicholson and Anthony Carlisle used the battery invented by Alessandro Volta for the electrolysis of water.



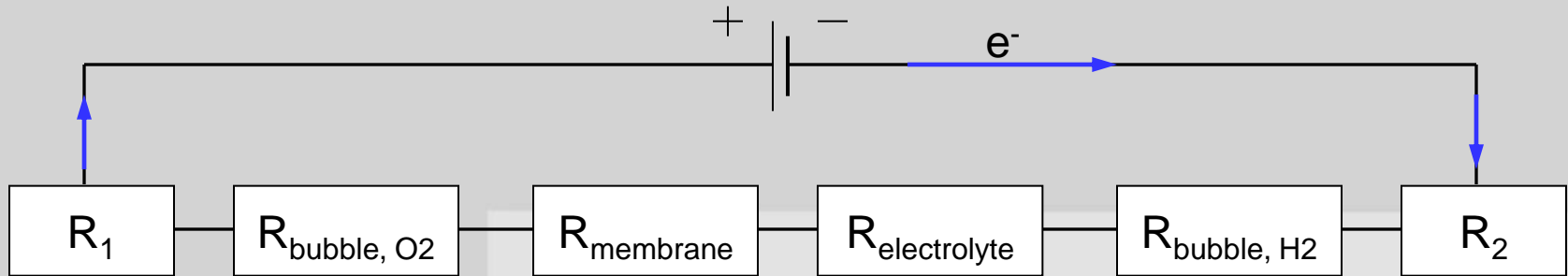
Overall reaction



$$\Delta E_{\text{cell}} = \Delta E^\circ + IR_{\text{cell}} + \Sigma \eta$$

Ways to reduce the cell voltage

$R_{cell} = \Sigma$ of external circuit resistance, electrolyte, membrane, bubbles



Minimize R

**High conductivity electrolytes
(acid or alkaline solutions)**

**Decrease wire length
Increase cross-section area
Conductive wire material**

Ways to reduce the cell voltage

$\Sigma\eta$ = activation overpotential + concentration overpotential

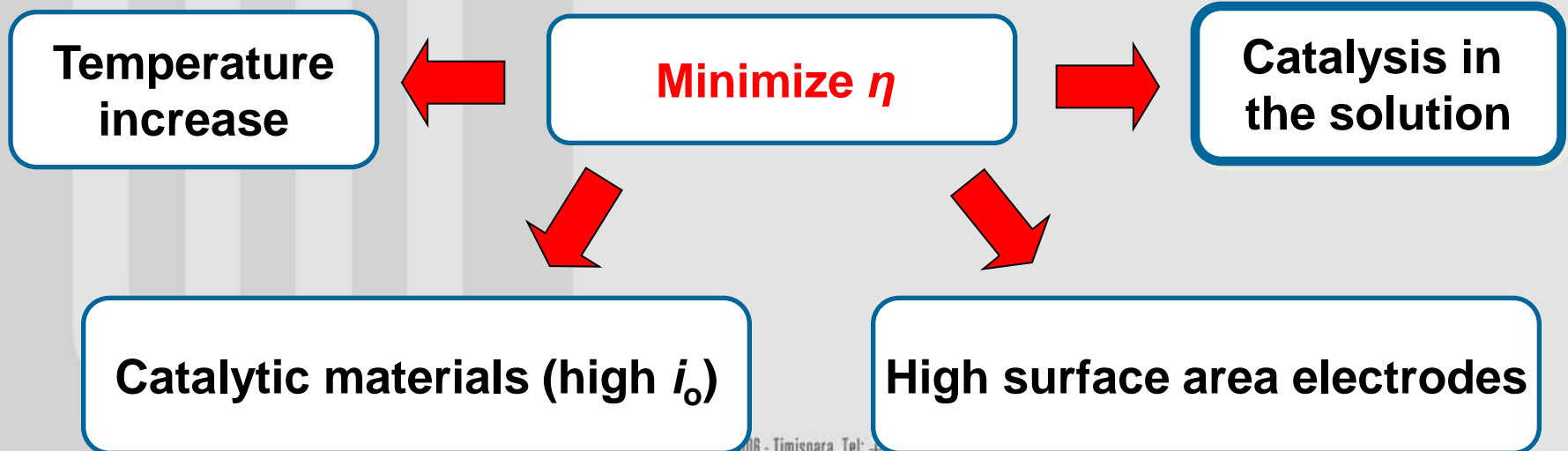
Electrode kinetics – Butler Volmer equation

$$i = i_o \left(e^{\alpha f \eta} - e^{-(1-\alpha) f \eta} \right)$$

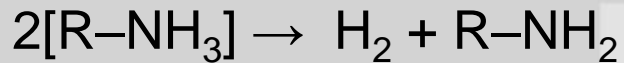
$$\eta = 2.303 \frac{RT}{(1-\alpha)F} \log i_o - 2.303 \frac{RT}{(1-\alpha)F} \log |i|$$

Tafel
equation

$$\eta = a + b \cdot \log |i|$$



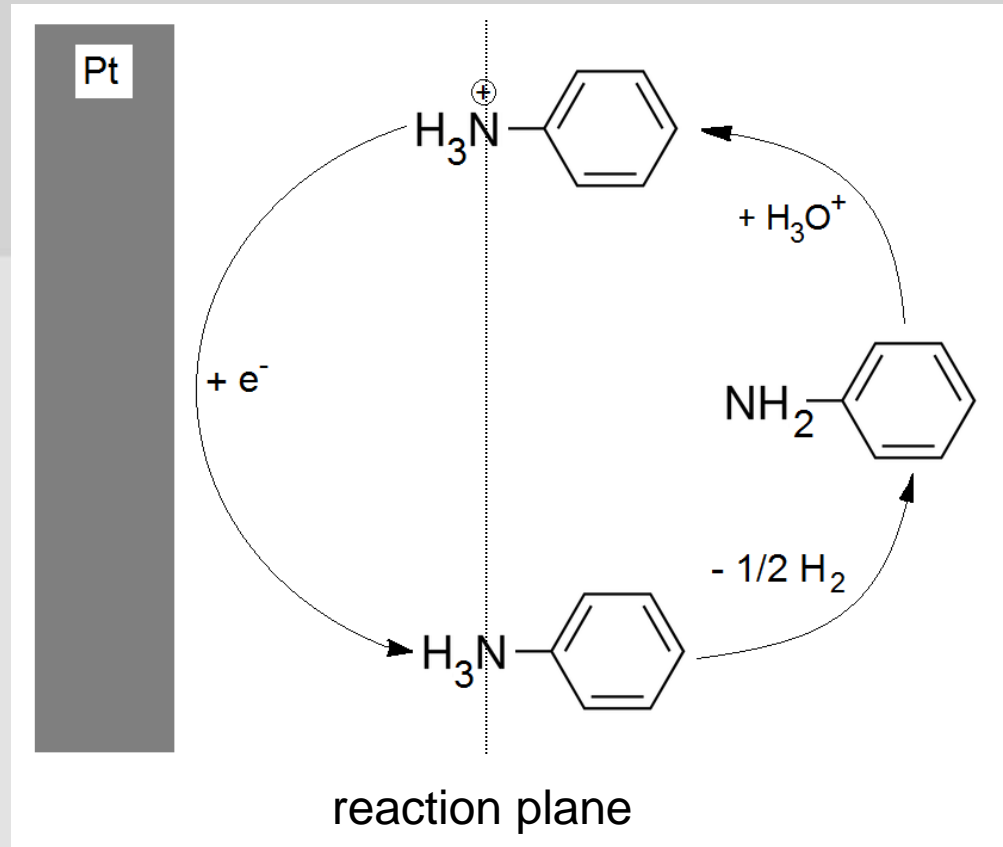
Catalysis by proton carriers



increase H^+ conc.



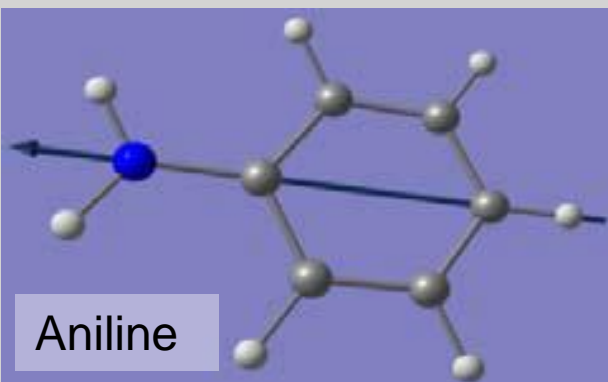
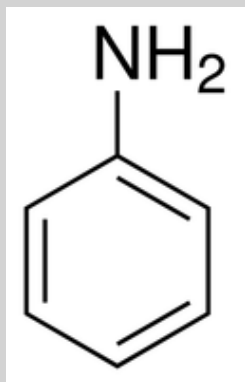
increased reaction rate



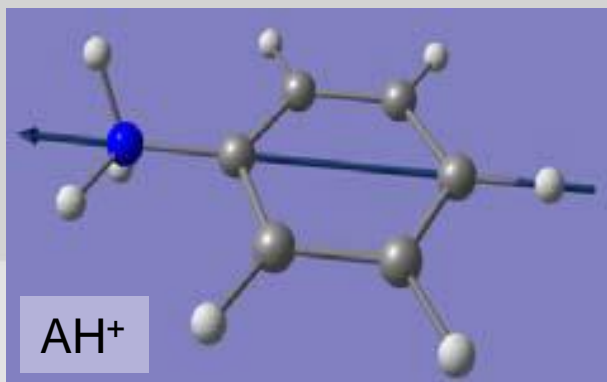
Proton carriers: aniline (A) & benzylamine (BA)

$\mu = 1.603 \text{ D}$

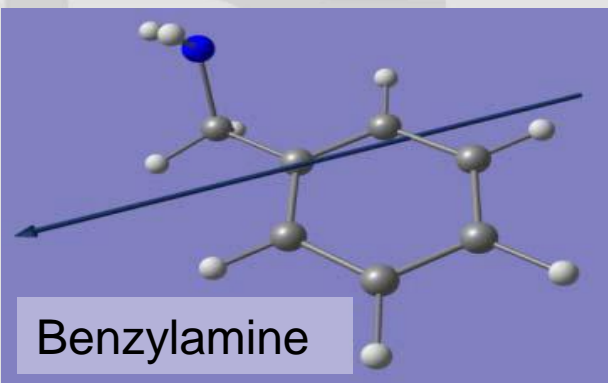
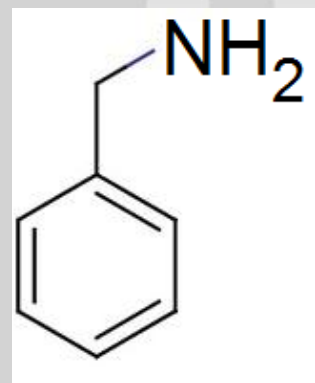
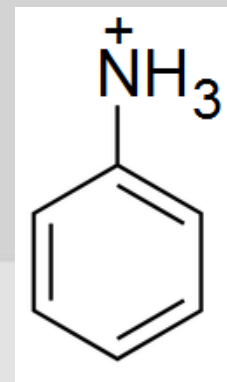
$\mu = 7.461 \text{ D}$



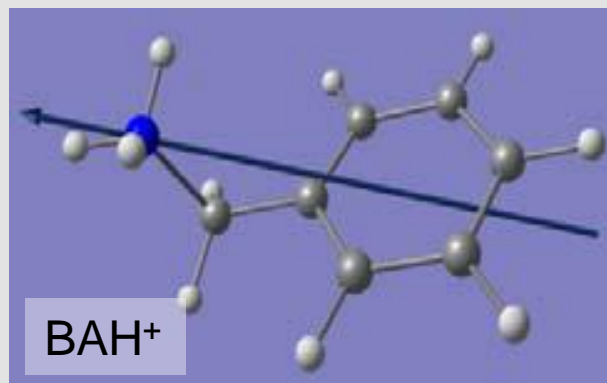
Aniline



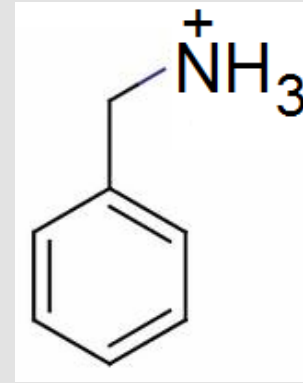
AH^+



Benzylamine



BAH^+



Dipole moment

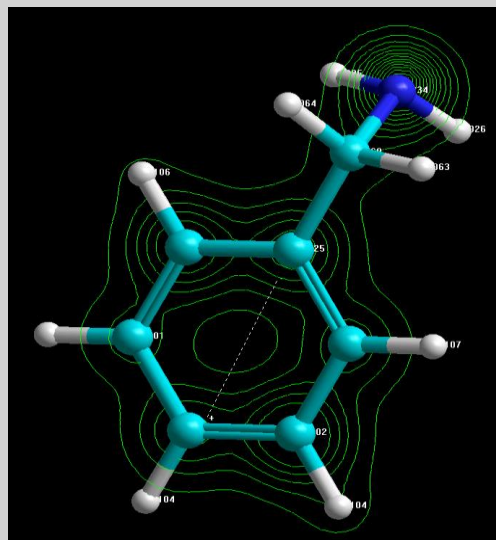
$\mu = 1.779 \text{ D}$

$\mu = 9.441 \text{ D}$

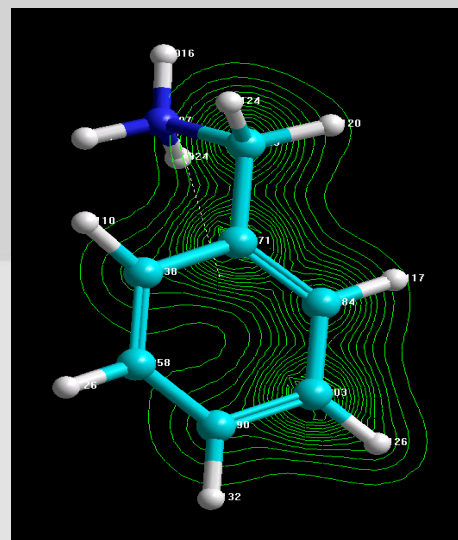
AH^+ = anilinium cation

BAH^+ = benzyl ammonium cation

Proton carriers: aniline & benzylamine



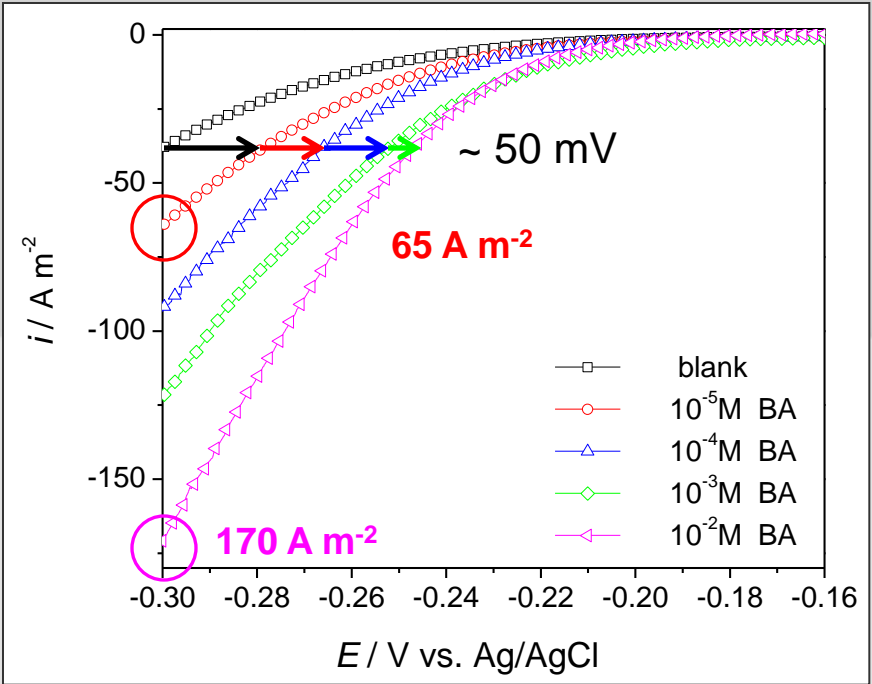
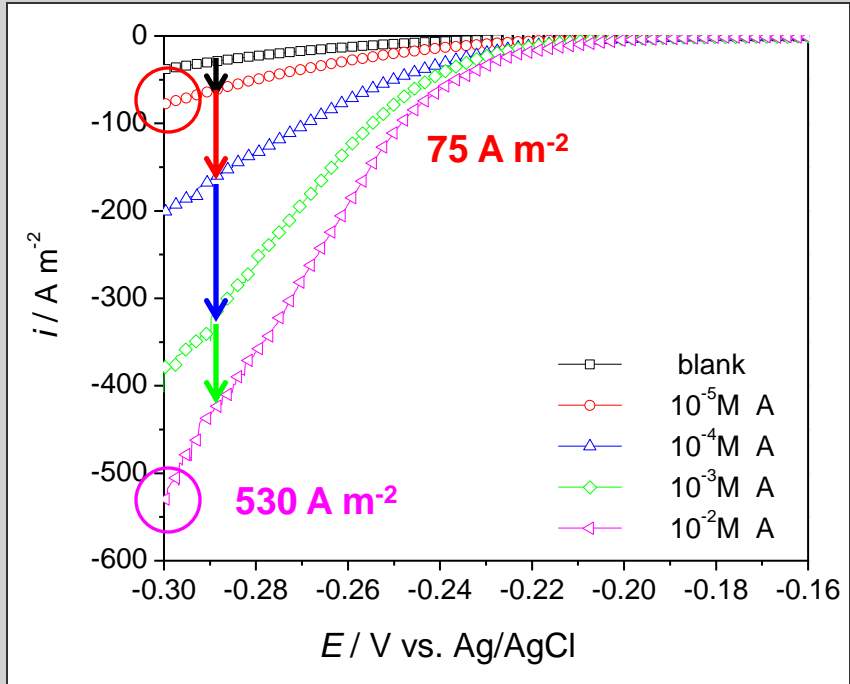
Benzylamine



Benzyl-ammonium

Electron densities of benzylamine and benzyl-ammonium molecules

Linear polarization curves



Low concentrations: comparable catalytic effect

High concentration: catalytic effect aniline \gg benzylamine

Tafel plots – kinetic parameters

$$\eta = 2.303 \frac{RT}{(1-\alpha)F} \log i_0 - 2.303 \frac{RT}{(1-\alpha)F} \log |i|$$

transfer coefficient

exchange current density

Tafel slope

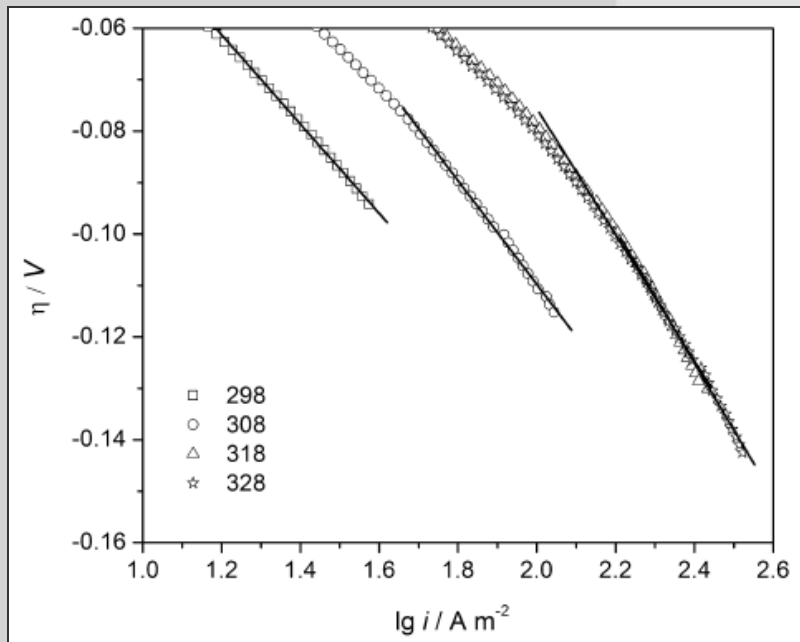


Table 1 – Kinetic parameters for HER in 0.5 mol L⁻¹ H₂SO₄ at different temperatures.

T [K]	$-b$ [mV dec ⁻¹]	$1-\alpha$	i_0 [A m ⁻²]
298	87	0.68	2.9
308	101	0.58	7.6
318	122	0.48	25.1
328	130	0.45	28.8

Tafel plots – kinetic parameters

 10^{-5} M

benzylamine

 10^{-2} M

Table 2 – Kinetic parameters for HER in 0.5 mol L⁻¹ H₂SO₄ with 10^{-5} M BA at different temperatures.

T [K]	-b [mV dec ⁻¹]	1 - α	i _o [A m ⁻²]
298	88	0.68	5.8
308	109	0.54	21.9
318	129	0.46	32.5
328	141	0.45	34.7

Table 3 – Kinetic parameters for HER in 0.5 mol L⁻¹ H₂SO₄ with 10^{-2} M BA at different temperatures.

T [K]	-b [mV dec ⁻¹]	1 - α	i _o [A m ⁻²]
298	103	0.57	22.9
308	119	0.49	41.7
318	129	0.45	51.3
328	140	0.42	66.1

Table 4 – Kinetic parameters for HER in 0.5 mol L⁻¹ H₂SO₄ with 10^{-5} M A at different temperatures.

T [K]	-b [mV dec ⁻¹]	1 - α	i _o [A m ⁻²]
298	94	0.63	6.9
308	100	0.59	11.0
318	121	0.45	28.2
328	136	0.43	40.7

Table 5 – Kinetic parameters for HER in 0.5 mol L⁻¹ H₂SO₄ with 10^{-2} M A at different temperatures.

T [K]	-b [mV dec ⁻¹]	1 - α	i _o [A m ⁻²]
298	110	0.54	67.6
308	126	0.47	128.8
318	147	0.40	169.8
328	168	0.35	239.9

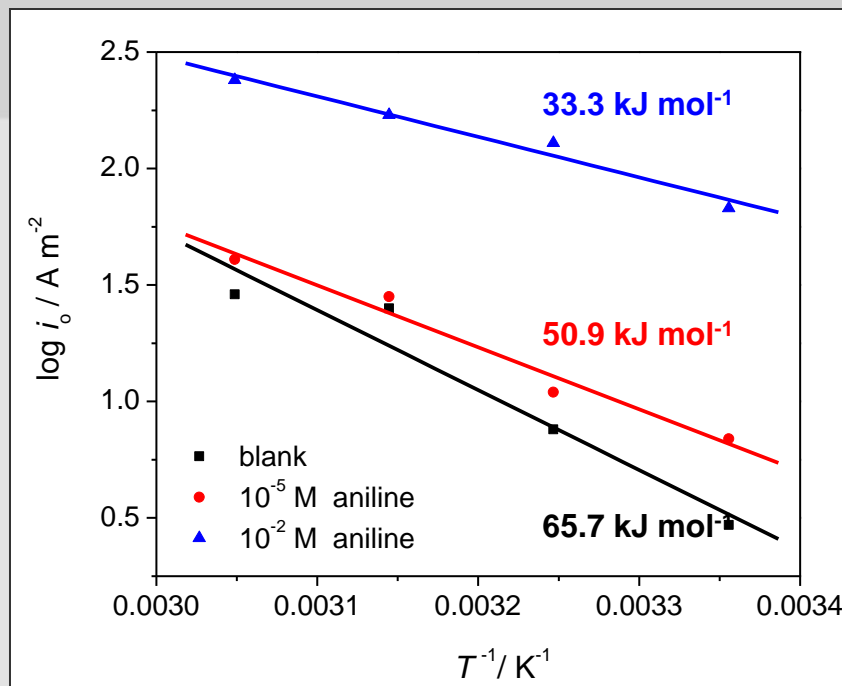
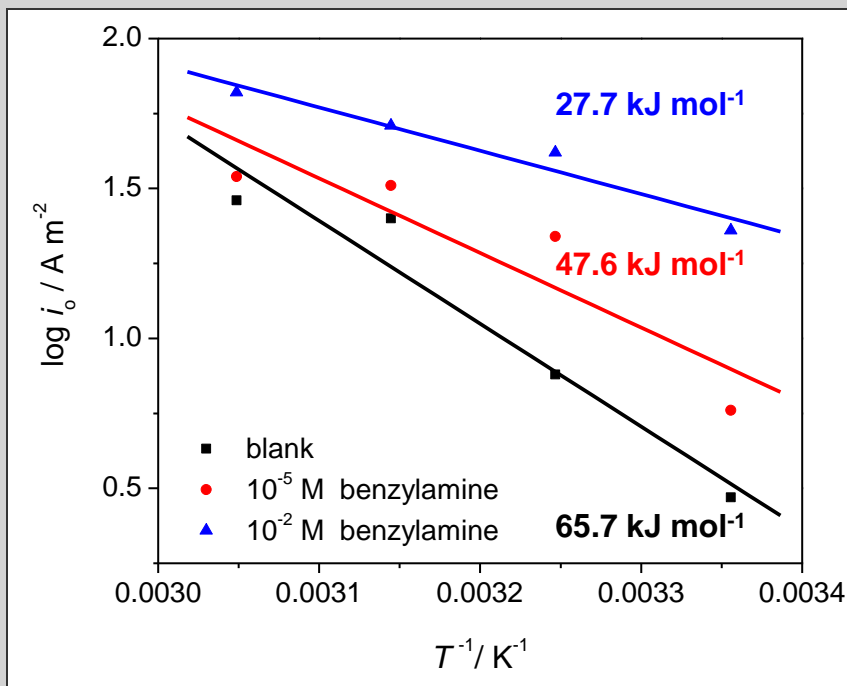
 10^{-5} M

aniline

 10^{-2} M

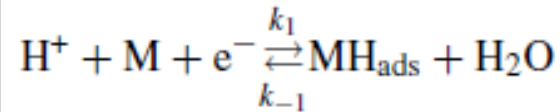
Apparent activation energy

$$E_a = -2.303 \frac{\partial(\log i_o)}{\partial(T^{-1})}$$

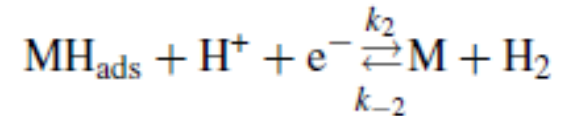


HER - mechanism

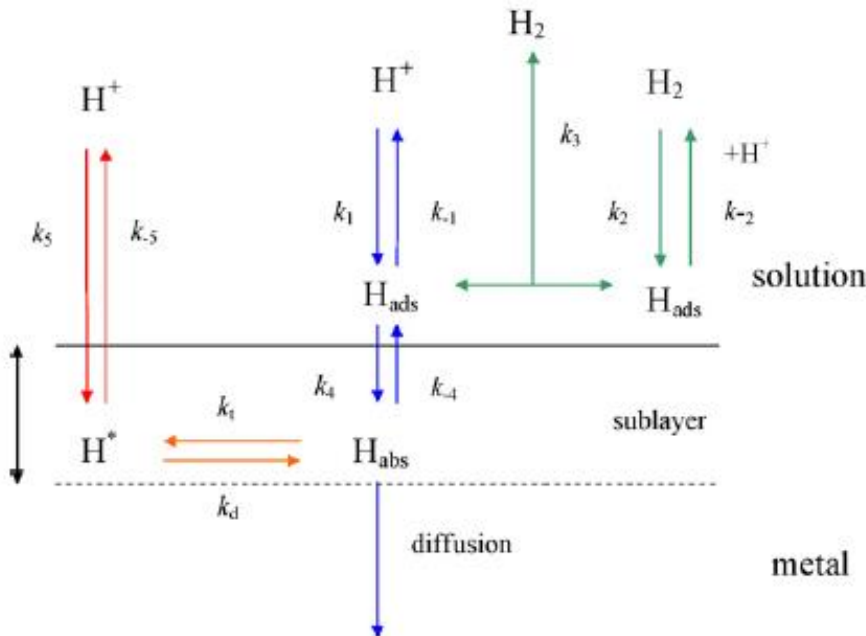
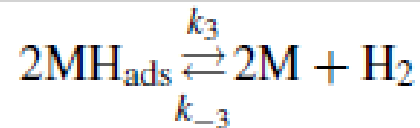
1. Volmer reaction - hydrogen adsorption

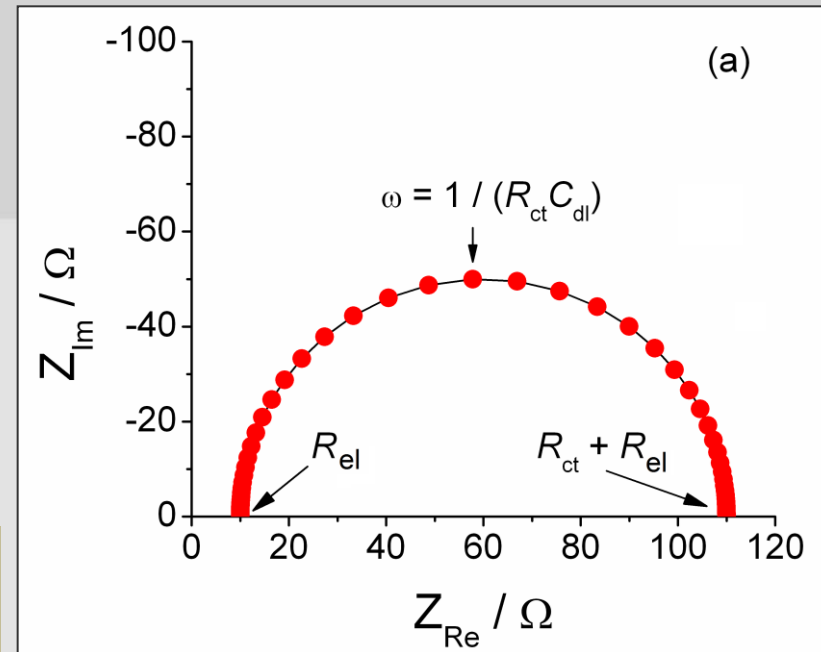
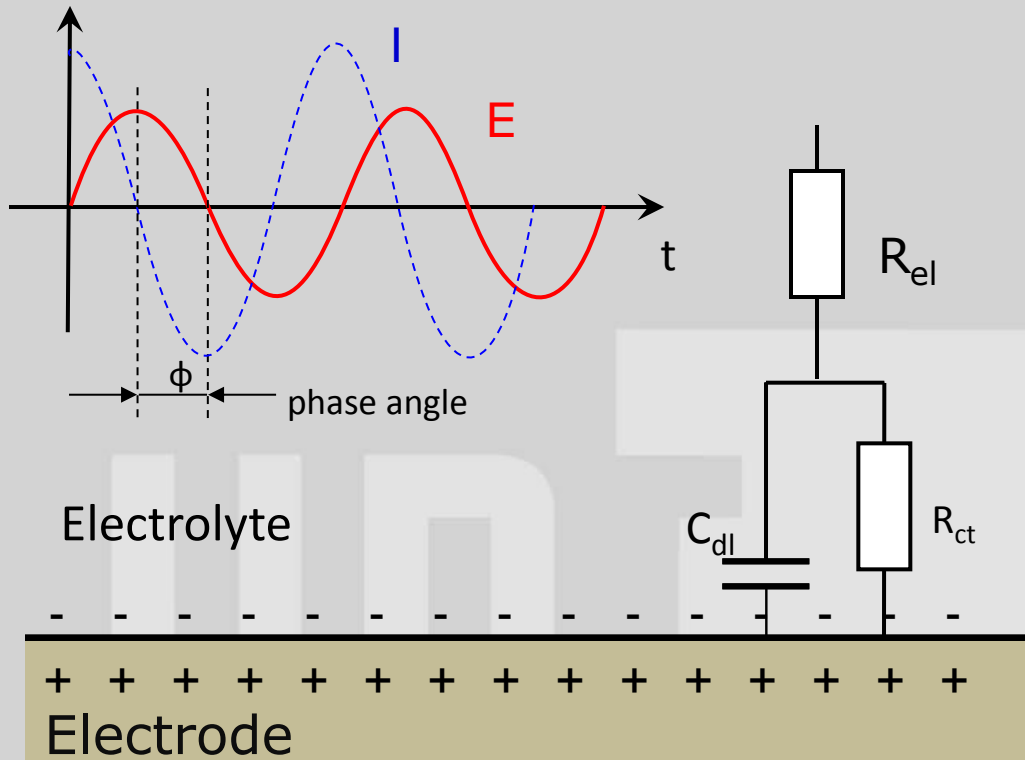


2. Heyrovsky reaction – electrochemical desorption



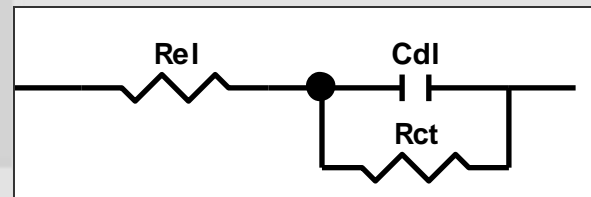
3. Tafel reaction – chemical desorption





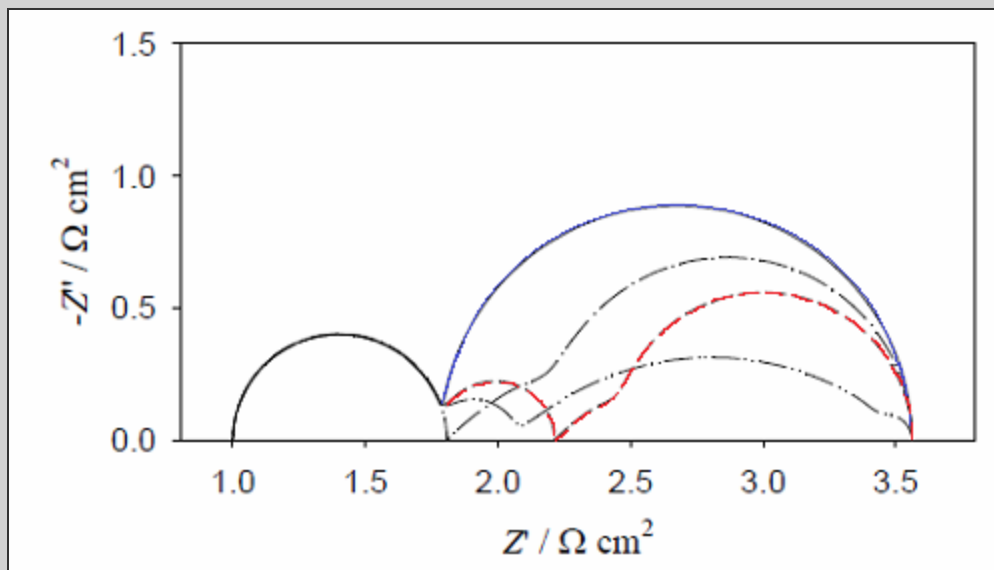
Nyquist plot

$$Z(j\omega) = R_{el} + \frac{R_{ct}}{1 + j\omega R_{ct} C_{dl}}$$

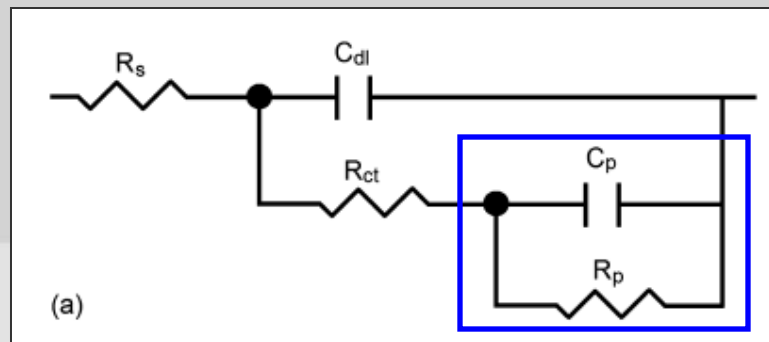


equivalent electrical circuit

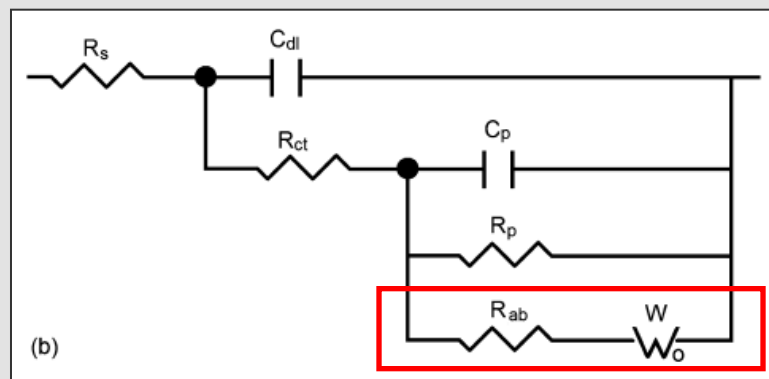
equivalent electrical circuit



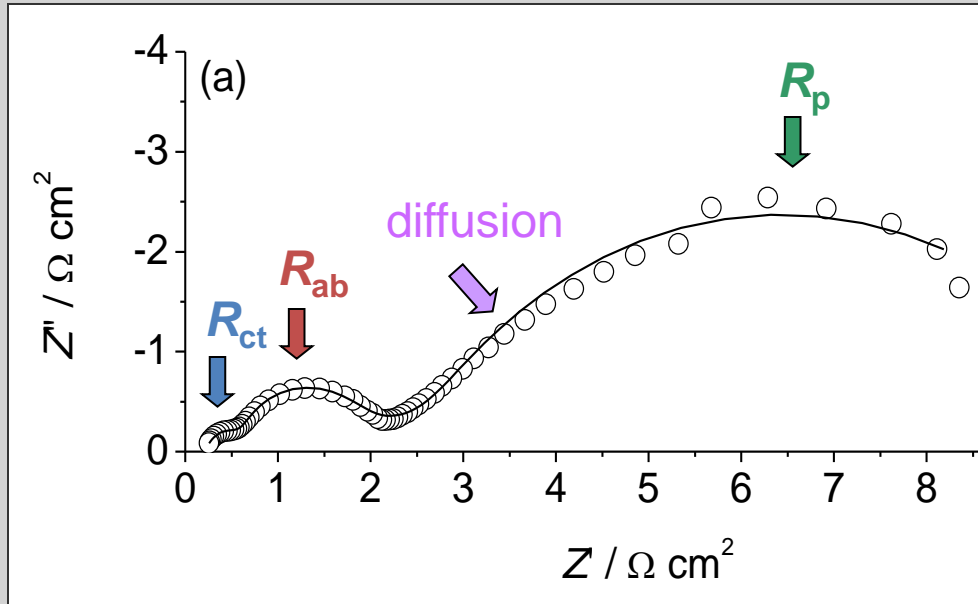
Simulated complex plane plots for HER



no hydrogen absorption



hydrogen absorption

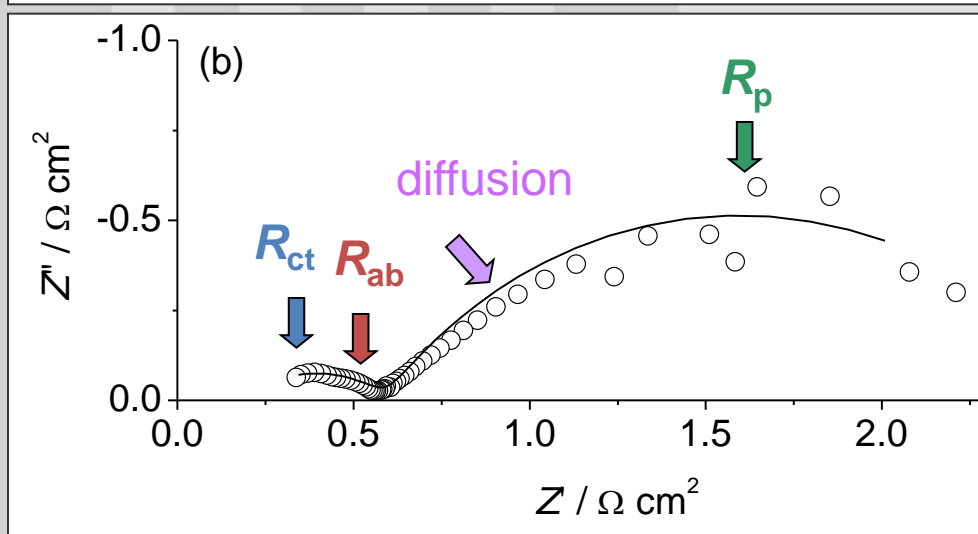


low η ($\eta = -0.25 \text{ V}$)

$$R_{ct} = 0.43 \Omega \text{ cm}^2$$

$$R_{ab} = 1.15 \Omega \text{ cm}^2$$

$$R_p = 9.76 \Omega \text{ cm}^2$$



high η ($\eta = -0.45 \text{ V}$)

$$R_{ct} = 0.15 \Omega \text{ cm}^2$$

$$R_{ab} = 0.06 \Omega \text{ cm}^2$$

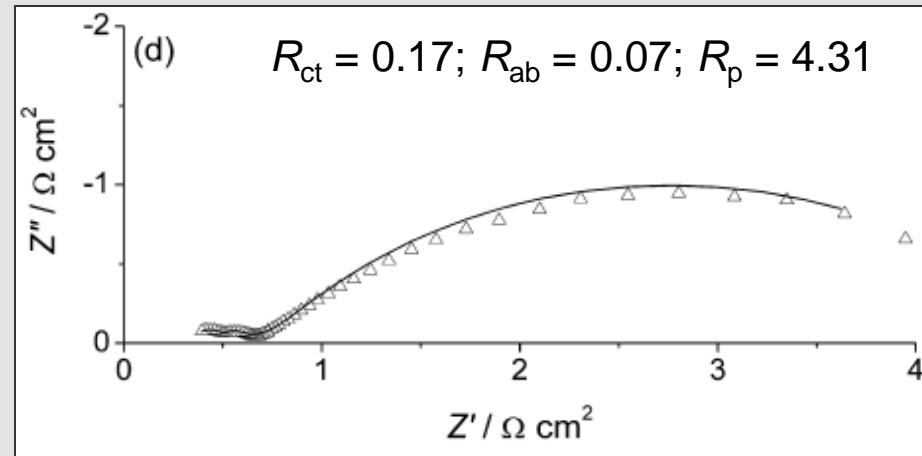
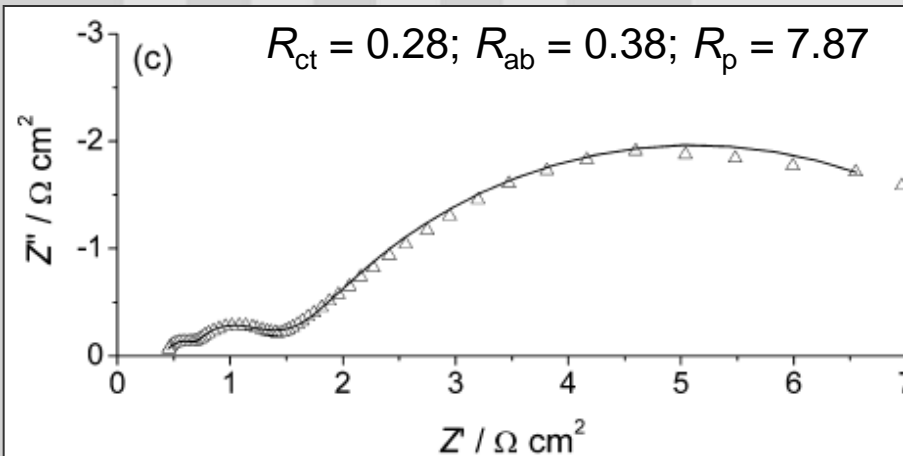
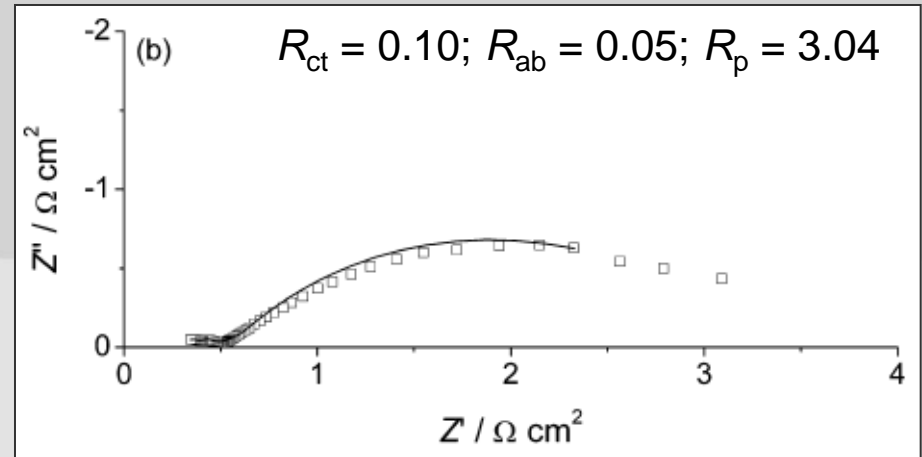
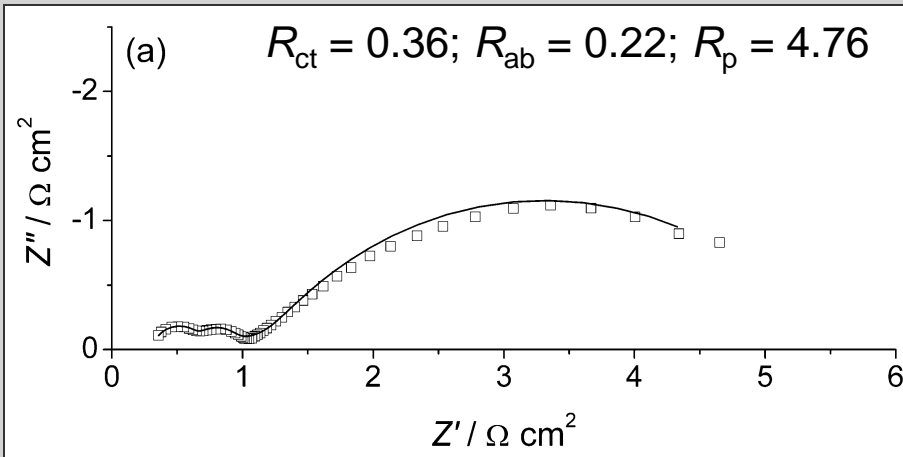
$$R_p = 2.06 \Omega \text{ cm}^2$$

Electrochemical impedance spectroscopy

10^{-5} M

benzylamine

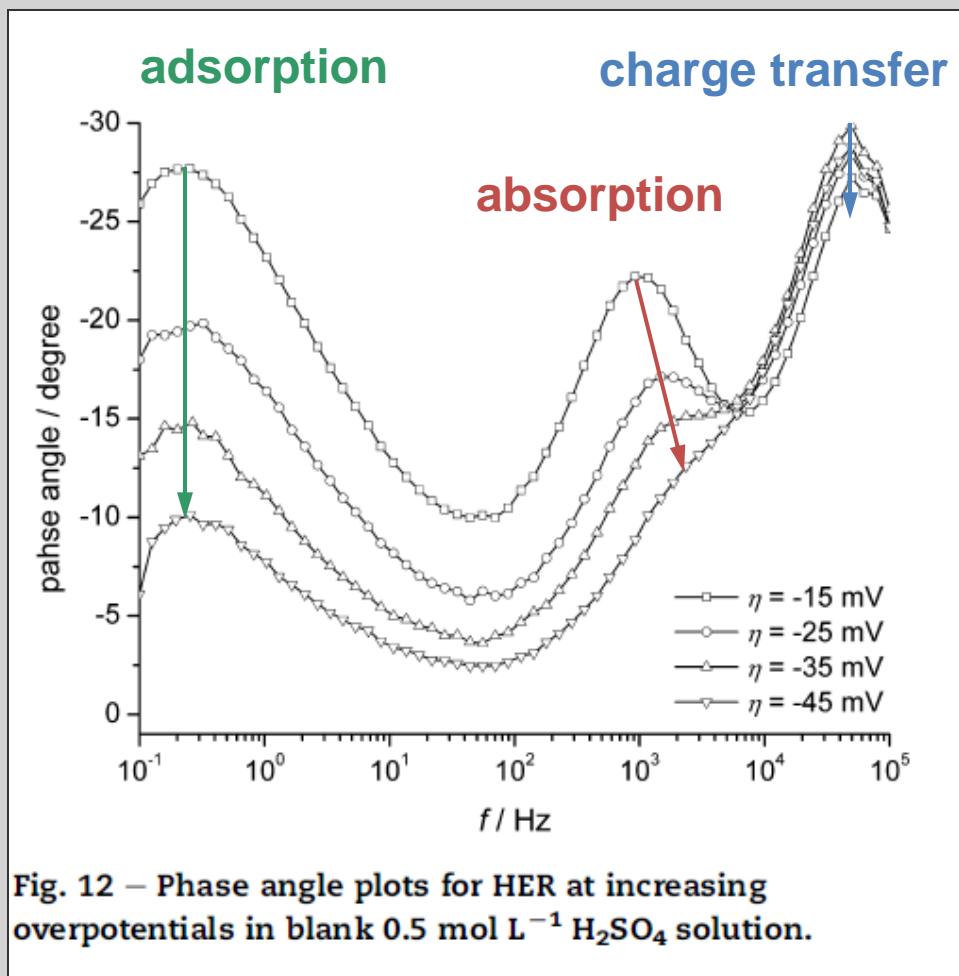
10^{-2} M



10^{-5} M

aniline

10^{-2} M



Charge transfer } potential independent
Adsorption }

Absorption – potential dependent

$\tau_{ct} = 9.2 \mu\text{s}$ → very fast

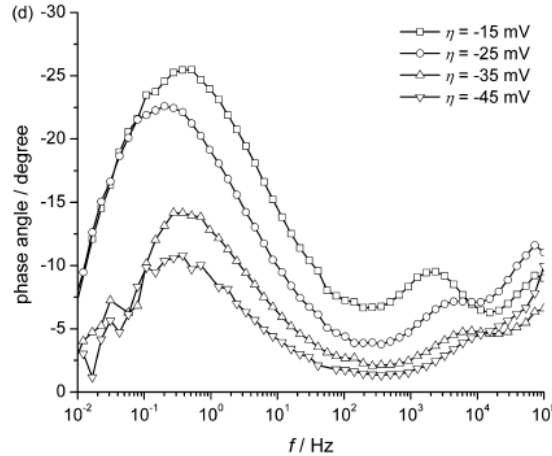
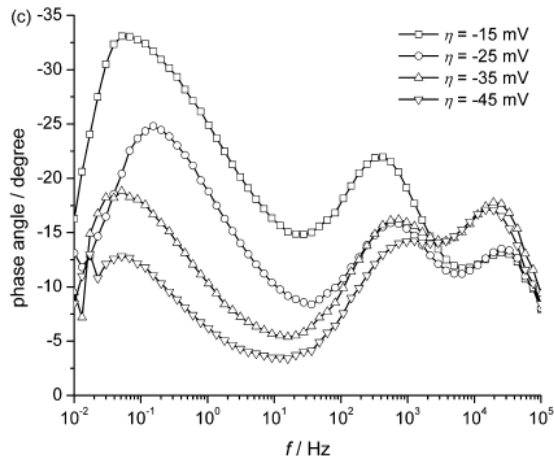
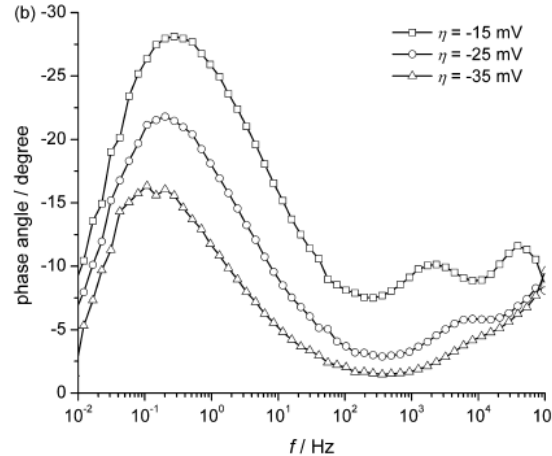
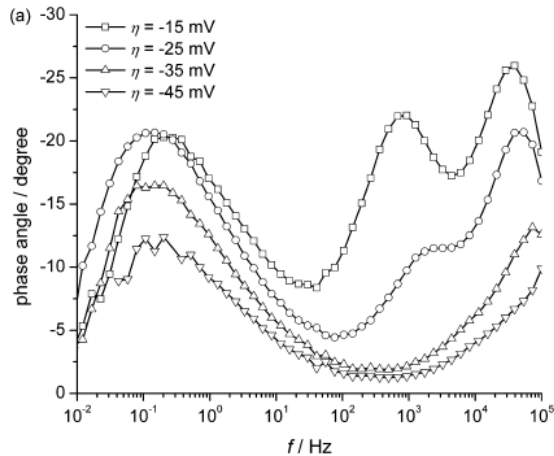
$\tau_{abs} = 0.255 \text{ ms}$ → fast

$\tau_{ads} = 2.17 \text{ ms}$ → slow

10⁻⁵ M

benzylamine

10⁻² M



10⁻⁵ M

aniline

10⁻² M

$$\tau_{ct} = 5.1 \mu\text{s} / 1.8 \mu\text{s}$$

$$\tau_{abs} = 0.063 \text{ ms} / 0.011 \text{ ms}$$

$$\tau_{ads} = 1.38 \text{ ms} / 0.72 \text{ ms}$$

$$\tau_{ct} = 8.0 \mu\text{s} / 2.5 \mu\text{s}$$

$$\tau_{abs} = 0.168 \text{ ms} / 0.018 \text{ ms}$$

$$\tau_{ads} = 3.49 \text{ ms} / 1.11 \text{ ms}$$

CONCLUSIONS

- HER is catalyzed by aromatic amines present in the solution;
- the amines increase the proton concentration at the metal-electrolyte solution interface due to the protonation of nitrogen atoms;
- the exchange current density values increase almost 10 times in the presence of benzylamine and more than 20 times in the presence of aniline;
- activation energy considerably drops in the presence of amines;
- kinetic parameters are strongly related to molecular parameters: dipole moment and molecular surface;
- impedance measurements showed that in the presence of amines HER is accelerated as a result of faster charge transfer resistance.

This work was partially supported by the project BS ERA.NET ID 31/2011: Hydrogen production from Black Sea water by sulfide-driven fuel cell (HYSUFCEL) which is gratefully acknowledged.

Phd. student Raluca Cretu

Prof. dr.eng. Nicolae Vaszilcsin

R. Cretu, A. Kellenberger, N. Vaszilcsin, Enhancement of hydrogen evolution reaction on platinum cathode by proton carriers, *International Journal of Hydrogen Energy*, 38 (2013) 11685-11694.



**THANK YOU
FOR YOUR ATTENTION!**